Image Cover Sheet

CLASSIFICATION	SYSTEM NUMBER 151648
UNCLASSIFIED	

TITLE

A SPATIAL TEMPORAL DYNAMICAL MODEL FOR MULTIPATH SCATTERING FROM THE SEA

System Number:

Patron Number:

Requester:

Notes:

DSIS Use only:

Deliver to:

A Spatial Temporal Dynamical Model for Multipath Scattering from the Sea

Henry Leung, *Member, IEEE*, and Titus Lo, *Member, IEEE*

Abstract—**A new method for modeling sea scattered signals is proposed in this paper. Instead of using a probabilistic model, a spatial temporal dynamical model is employed to model the sea scatter phenomenon. Our approach is empirical in the sense that a model is constructed based on experimental data. We extend the approach of using a temporal predictor for temporal dynamical system reconstruction to a spatial temporal predictor for reconstructing a spatial temporal one. The basic spatial temporal dynamical model used in this study is a couple map lattice (CML) rather than the conventional partial differential equation. The Radial Basis Function (RBF) neural network is incorporated into the CML to enhance the function approximation ability, and the autocorrelation function is used to determine the spatial effect across individual channel. An array antenna was used to collect real spatial temporal sea scattered data for this study. Preliminary results shows that the new model provides an accurate description of the sea scattered signals, and has the potential for signal processing applications.**

I. Introduction

THE problem of scattering from a rough surface has become of special interest for many years. It arises in many subjects such as radio communications, tropospheric propagation, radio astronomy, acoustics and radar surveillance [1]–[3]. Conventional rough surface scattering models [4], [5] are basically concentrated on the statistical characteristics of the scattered signals. Statistical models are used instead of the scattering equation because statistical model can provide an easy tool for signal processing applications. The analysis of the distribution of the scattered field is based upon the assumption of many independent scatterers in the illuminated patch. In the limit of a large number of scatterers, the amplitude of the scattered field is Ricean distributed. In case where the contributing area of the surface resolves the gross sea wave structure, an approach similar to that used earlier for bunching of scatterers leads to the generalized K-distribution [6].

In this paper we address the problem of rough surface scattering by constructing models directly from experimental data. We expand an earlier work reported in [7], in which we developed a temporal dynamical model for sea scattered signals. Rather than using the conventional stochastic model, we attempt to construct a nonlinear dynamical model for sea scattered signal instead. We measured the correlation dimension and local divergence of real sea scattered signals. Both tests gave us positive results which indicate that a sea scattered signal may possibly be modeled as a nonlinear dynamical system. That is, finite fractional dimension and exponential divergence. We then used the local prediction method [8] to reconstruct the dynamics of sea scattered signal, and fairly good recursive prediction results were obtained. We concluded in [7] that chaos may provide a good mathematical tool for modeling sea scattered signals, especially for signal processing applications [9], [10].

While chaos has a strictly temporal meaning, it assumes that the spatial structure remains frozen. This leads us to a new limitation of the dynamical systems approach: What happens when the degrees of freedom have an undoubtedly spatial significance? Chaos is a ubiquitous phenomenon widely observed in dynamical systems with a sufficient degree of nonlinearity. If, in addition, the system considered is spatially extended with effectively many degrees of freedom, we use the term spatial-temporal chaos [11]. Spatial-temporal chaos is observed in a wide range of systems, particularly hydrodynamical systems. For sea scattered signal, spatial effects cannot be ignored. In fact, sea scattered signals in nearby area are strongly correlated since the scattered signals come from a moving surface. Furthermore, the mathematical model for scattering, provides a mathematical basis that scattering is a spatial temporal phenomenon.

It is the purpose of this paper to develop a spatial-temporal model for sea scattered signals. Instead of developing a purely temporal dynamical system, we attempt to construct a spatial-temporal predictive model directly from the experimental time and space series data. In Section II, we describe the radar system used in the experiment and the properties of the sea scattered data collected in a field trip. Spatial correlation analysis of the data is presented to illustrate the spatial effect of the scattered signal. In Section III, a special type of spatial temporal dynamical system called coupled map lattice (CML) is described. We combine the CML with a Radial Basis Function (RBF), which is a powerful technique in predicting chaotic time series, to extract the spatial temporal pattern of sea scattered signals. The experimental analysis is reported in Section IV.

II. The Experimental Data

We begin with a description of the experimental apparatus and then a description of the data. The data used in this paper were collected in a field trip which was performed on the east coast of the Bruce Peninsula, Ontario, Canada, overlooking Lake Huron. This particular location was chosen

Manuscript received August 4, 1993; revised September 15, 1994.

H. Leung is with the Radar and Space Division, Defence Research Establishment Ottawa, Ottawa, ON K1A 0K2, Canada.

T. Lo is with the Communications Research Laboratory, McMaster University, Hamilton, ON L8S 4K1, Canada.

IEEE Log Number 9408756.

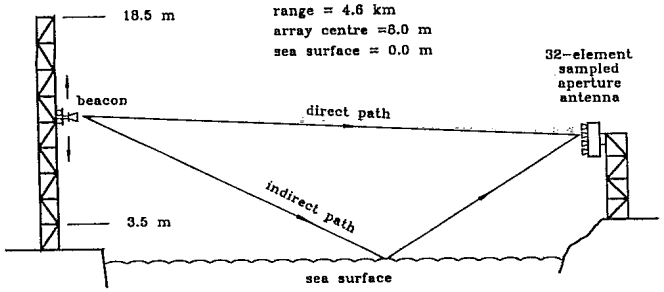

Fig. 1. The experimental setup and measurement geometry on Lake Huron.

because of the high sea states caused by the combination of the westerly winds, the shallow water offshore, and the long fetch across Lake Huron. One of the objectives of the experiments was to acquire data suitable for studying electromagnetic waves scattered from an ocean surface. A 32-element sampled aperture antenna was used to collect scattering data under a variety of meteorological and water surface conditions. The experimental system consisted of a transmitter, a sampled aperture antenna, and a data acquisition system. The transmitter was a 100-mW CW beacon, sited at a distance of 4610 metres from the receiving antenna. Fig. 1 gives a vertical view of the geometry of the measurement setup. It should be stressed that although the spatial dimension in our problem is the vertical positions of the receiving horns, the spatial information which is being added to the temporal data is really horizontal sea surface information. The height of the transmitting horn could be varied through the height interval from 3.5 to 18.5 metres above the water level. The receiving antenna array has a 1.82-metre aperture and consists of 32 10-dB Horizontal-polarized horns. All elements in the array were precisely aligned and uniformly distributed to within 0.1 mm to minimize errors due to misalignment. The array was fixed at 8.8 metres above the water level. I and Q samples were acquired from each of the 32 elements at a sampling rate of 62.5 samples/second, 12-bit precision, and then were recorded onto the storage media. The system operated at two X-band frequencies simultaneously. One of the frequency channels was kept fixed at 10.2 GHz throughout the entire measurements, while the other was switched in an agile fashion from 8 GHz to 12 GHz in 300 MHz steps. The number of samples in a typical data set was 127 for each of the 32 elements. A typical spatial-temporal sea scattering data set collected by the array radar is depicted in Fig. 2. Note that the amplitude of the signal used in this paper is scaled. The dynamic range of the A/D is -5 V to 5 V with 12-bit quantization levels. We scale the amplitude by 100. Therefore, if the amplitude is 10, then the signal should be 2.4 V. In other words, the amplitude used here represent the strength of the field, proportionally. In Fig. 2, the five array outputs are shifted by 2.5 to have a clear depiction of the waveforms.

The spatial correlation functions are formed by evaluating the cross-correlation coefficients between the signals at the array elements. That is, the spatial correlation function is given by

$$\Phi(i,j) = \frac{R_{ij}}{\sqrt{R_{ii}R_{jj}}} \qquad \text{for } i = 1,\cdots,M, j = 1,\cdots M \quad (1)$$

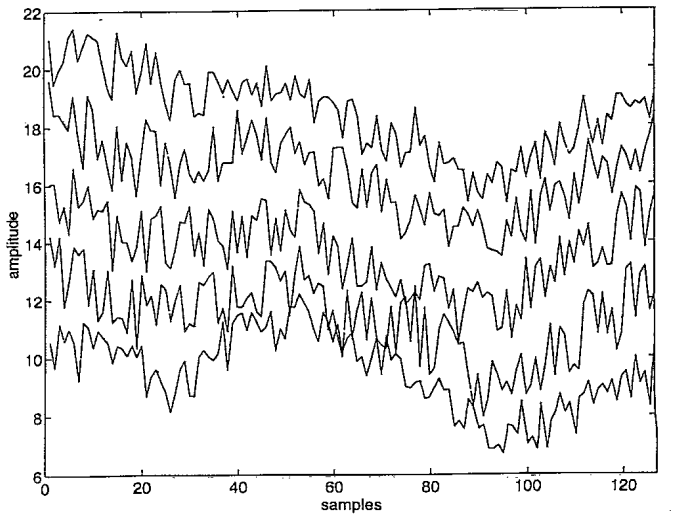

Fig. 2. Typical waveform of sea scattered signals collected by five sensors on the array antenna.

where M is the number of array elements, R_{ij} is the cross correlation function between $x_i(t_n)$ and $x_j(t_n)$, and $x_i(t_n)$ is the signal at the ith element at time t_n. Since a vertical array was exclusively used in this study, the spatial correlation information is limited therefore to the vertical direction. Intuitively, it is expected that the greater the separation between the antenna elements, the smaller the correlation between the signals from these elements. Fig. 3(a) and (b) give the time history of the signals from the two adjacent elements of the array. The separation of these two elements is 0.05715 m. There is a strong similarity between the signals. In fact, the correlation coefficient for these two signals is 0.8. On the other hand, it is observed that signals from two elements that are separated by 1.82 m bear little resemblance to one another, as shown in Fig. 4(a) and (b). In this case, the spatial correlation coefficient is 0.18. The spatial correlation coefficient, as a function of antenna separation is given in Fig. 5, where the solid line represents the spatial correlation function for 8.05 GHz, the dashed line represents the function for 10.12 GHz, and the dot-dashed line represents the function for 12.22 GHz. It can be observed that the magnitude of the spatial correlation coefficients for all the frequencies decreases as the antenna separation increases. This relationship is shown in Fig. 6, which is derived from a number of data sets which were recorded at different frequencies. This spatial correlation analysis implies the need of a spatial temporal model for sea scattered signals.

III. Coupled Map Lattice Using Radial Basis Function

The model used to study the spatial-temporal dynamics of EM scattering from an ocean surface in this paper is a coupled map lattice (CML) [12], which has been recently investigated extensively in various contexts. The coupled map lattices have the advantage over partial differential equations that many of the technical problems associated with existence, uniqueness etc are absent so that the essential problems of spatial-temporal chaos are as transparent as possible [13]. Coupled map lattice models are constructed by supposing

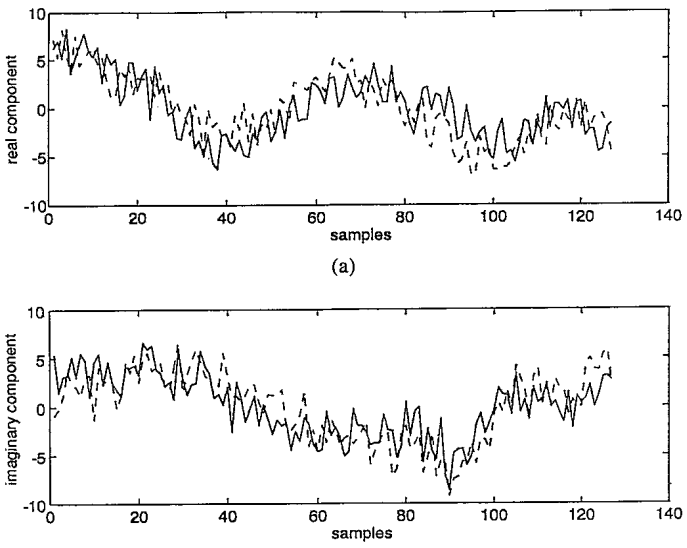

Fig. 3. A comparison of signals at two adjacent elements of the 32-element array. $f = 10.2$ GHz. (a). In-phase component and (b) quadrature-phase component.

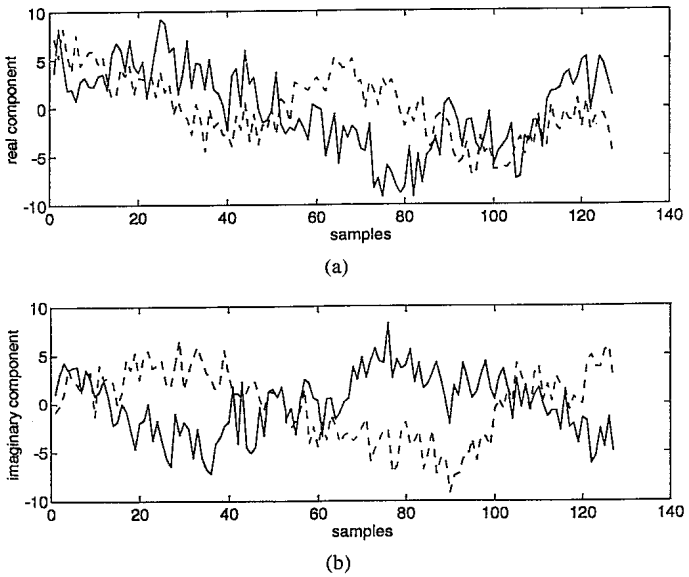

Fig. 4. A comparison of signals at the bottom and top elements of the 32-element array. $f = 10.2$ GHz. (a) In-phase component and (b) quadrature-phase component.

that a set of local discrete-time dynamical elements occupy the sites of some lattice and interact with each other. There are various ways to introduce coupling between neighboring elements. Basically, a coupled map lattice is a dynamical system with discrete time, discrete space, and continuous state. The simplest coupled map lattices are mappings of the form

$$x_{n+1}(i) = \sum_{j=-\infty}^{\infty} k_\varepsilon(i,j) f(x_n(j)) \tag{2}$$

where f is a differentiable mapping on a vector space Y and k_ε: $\mathbb{I} \times \mathbb{I} \to \mathbb{R}$ is a function depending continuously on $\varepsilon \in \mathbb{R}$.

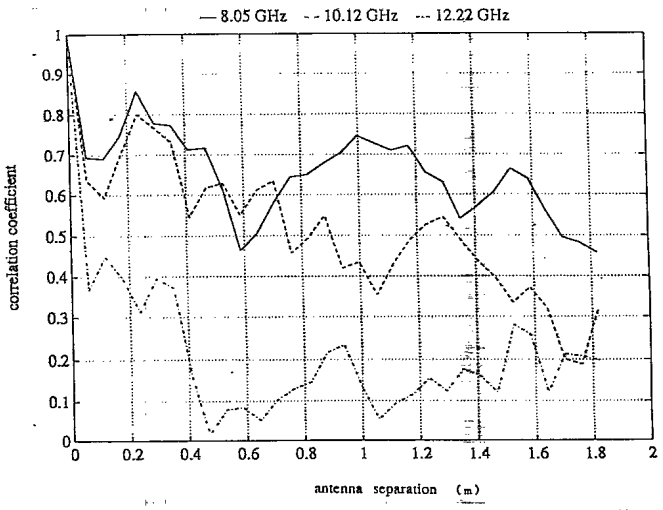

Fig. 5. A comparison of spatial correlation functions for three different frequencies.

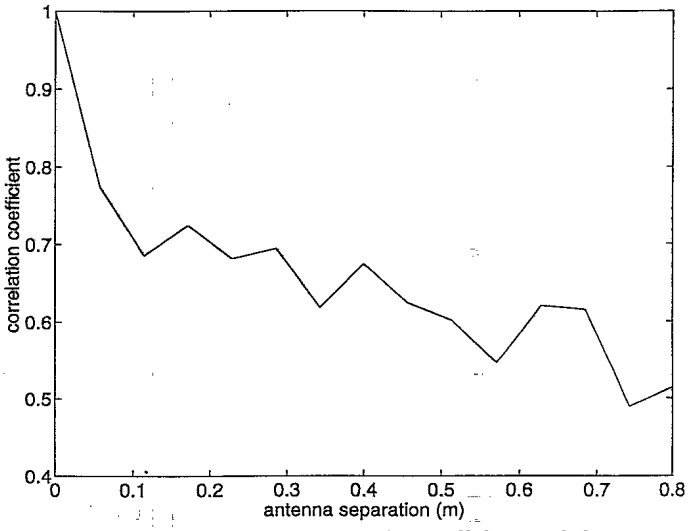

Fig. 6. Relationship between the correlation coefficients and the antenna separation.

We assume that the k_ε are nonnegative and satisfy for all $i \in \mathbf{N}$

$$\sum_{j=-\infty}^{\infty} k_\varepsilon(i,j) = 1. \tag{3}$$

We shall demand that k_ε is translation invariant so that

$$k_\varepsilon(i,j) = s_\varepsilon(|i-j|) \tag{4}$$

and often, in addition, that this interaction is exponentially decaying in the sense that s_ε satisfies

$$\begin{aligned} &s_\varepsilon(i) \le C \exp(-ai), \\ &s_\varepsilon(i) \le \varepsilon \qquad \text{for all } i \in \mathbf{N}, \\ &s_\varepsilon(0) \in [1-\varepsilon, 1] \end{aligned} \tag{5}$$

for some constants $a, C > 0$.

A much studied class of such coupled map lattices is given for $Nh \in \mathbb{I}$ by choosing $s_\varepsilon = s_\varepsilon^{(Nh)}$ in (4) as follows:

$$s_\varepsilon^{(Nh)}(n) = \begin{cases} 1-\varepsilon & \text{for } n = 0 \\ \dfrac{\varepsilon}{2n} & \text{for } 0 < n \le Nh \\ 0 & \text{otherwise} \end{cases} \tag{6}$$

where Nh is the neighborhood. When $Nh = 0$, it means that the dynamical system is purely temporal. The stronger the spatial effect, the larger Nh should be used. The simplest mapping of this family, the one for nearest neighbour coupling ($Nh = 1$), has been studied extensively, in particular with the help of computers [13]. The one-dimensional lattice, which is the combination of local nonlinear process and diffusion, can be seen in the reaction-diffusion system. As the independent units, we take local nonlinear process $x(i) \to x'(i) = f(x(i))$, and the discretized diffusion process $x'(i) \to (1-\varepsilon)x'(i) + \varepsilon/2[x'(i+1) + x'(i-1)]$. Combining these two procedures, our dynamics can be written as

$$\begin{aligned} x_{n+1}(i) = &(1-\varepsilon) f(x_n(i)) \\ &+ \frac{\varepsilon}{2}[f(x_n(i+1)) + f(x_n(i-1))] \end{aligned} \tag{7}$$

where n is a discrete-time step, i is a lattice point, and ε is a small parameter which specifies the strength of coupling.

In (7), the independent procedures are local transformation f, and the diffusion process, which are separated parallel procedures. The model consists of the sequential repetitions of these two procedures. This argument leads to the following equivalent form

$$x_{n+1}(i) = f((1-\varepsilon)x_n(i) + \frac{\varepsilon}{2}(x_n(i+1) + x_n(i-1))) \tag{8}$$

with the above model [13]. At present, the most extensive simulations of coupled lattice maps are those carried out in [13], which investigated (8) with the special case of the logistic map

$$f(x) = \lambda x(1-x) \tag{9}$$

which demonstrates the infinite sequence of period doubling bifurcation. As the nonlinearity λ is increased, the single logistic map shows the classic period doubling cascade to chaos. In the lattice equation, this local temporal period doubling induces spatial domain structures of phase coherent sites.

Although the logistic map generates rich dynamical behavior, it is seldom used for time series prediction because of its limited function approximation ability. Recently there has been a great deal of interest in reconstructing a dynamical system from a chaotic data sequence [14], [15]. Different approaches such as multilayer neural network [14], radial basis function [15], local method [8] and genetic algorithm [16] are investigated. While these approaches have their own advantages and weaknesses, they all have a common property that they are universal approximators. That is, they can approximate any continuous function arbitrary closely by choosing a suitable structure and parameters. In this paper, the radial basis function (RBF) is chosen for the nonlinear local transformation f.

Given a set of data $\{(\boldsymbol{x}_i, y_i) \in \mathbb{R}^n \times \mathbb{R} | i = 1, \cdots, N\}$, the RBF corresponds to choosing the form of the interpolating function as

$$y_j = \sum_{i=1}^{N} w_i h(\|\boldsymbol{x_j} - \boldsymbol{x_i}\|^2) \qquad j = 1, \cdots, N \tag{10}$$

where h is a smooth univariate function defined on $[0, \infty)$, w_i are weighting functions and $\|\cdot\|$ is a norm on $\mathbb{R}^n$. This formula means that the RBF is expanded on a finite N-elements basis that is given from the set of functions h translated and centered at data points. Defining the vectors $\boldsymbol{y}, \boldsymbol{w}$ and the symmetric matrix $\boldsymbol{H}$ as follows:

$$\begin{aligned} &\boldsymbol{y} = (y_1, y_2, \cdots, y_N)^T, \quad \boldsymbol{w} = (w_1, w_2, \cdots, w_n)^T, \\ &(\boldsymbol{H})_{ij} = h(\|\boldsymbol{x_i} - \boldsymbol{x_j}\|^2) \end{aligned} \tag{11}$$

we obtain

$$\boldsymbol{w} = \boldsymbol{H}^{-1}\boldsymbol{y} \tag{12}$$

provided $\boldsymbol{H}$ is invertible. The invertibility of $\boldsymbol{H}$ depends on the choice of the function h. The most widely used function should be the Gaussian function $e^{-(\|\cdot\|/\sigma)}$, which has been proved to provide an invertible $\boldsymbol{H}$ [17].

One reason for using a Gaussian function is that RBF and regularization has interesting connections when the basis functions are chosen to be Gaussian. If the data are noisy, a well known regularization technique is to substitute (12) with the following

$$\boldsymbol{y} = (\boldsymbol{H} + \lambda \boldsymbol{I})\boldsymbol{w} \tag{13}$$

where λ is a small parameter and $\boldsymbol{I}$ is the identity matrix. The same approximating function can be obtained from a pure regularization approach. Let us consider the following functional:

$$\sum_i (\boldsymbol{y} - \boldsymbol{f}(\boldsymbol{x_i}))^2 + \lambda \int \sum_{k=0}^{\infty} \boldsymbol{a}_m (D^m \boldsymbol{f}(\boldsymbol{x_i}))^2 \, \boldsymbol{dx} \tag{14}$$

where λ is a parameter, $D^{2m} = \nabla^{2m}, \nabla^2$ is the Laplacian operator and the coefficients a_m are to be chosen. It has been proven [18] that by posing $a_m = \sigma^{2m}/m!2^m$ the function that minimizes this functional can be written as

$$\boldsymbol{f}(\boldsymbol{x}) = \sum_{i=1}^{N} w_i \boldsymbol{G}(\|\boldsymbol{x} - \boldsymbol{x_i}\|^2) \tag{15}$$

where $\boldsymbol{G}$ is a Gaussian of variance σ and the coefficients satisfy the linear system (13) with $(\boldsymbol{H})_{ij} = \boldsymbol{G}(\|\boldsymbol{x_i} - \boldsymbol{x_j}\|^2)$. So in this case RBF and regularization are equivalent. Since dynamical system reconstruction is an inverse problem which is ill-posed, an approximation scheme with regularization ability is highly desirable.

The CML of (8) is usually used with the logistic map (9), and hence the future state of the system x_{n+1} depends only on the present state x_n. However, the embedding dimension cannot be restricted to unity for dynamical system reconstruction or time series prediction. In this case, the CML becomes

$$x_{n+1}(i) = f((1-\varepsilon)\boldsymbol{x_n}(i) + \frac{\varepsilon}{2}(\boldsymbol{x_n}(i+1) + \boldsymbol{x_n}(i-1))) \tag{16}$$

where $\boldsymbol{x}_n$ is the d-dimensional state vector at time n, which is equal to $(x_n, x_{n-1}, \cdots, x_{n-D+1})$ and d is the embedding dimension of the process. Substituting the Gaussian RBF into (16), we have a couple RBF lattice given as

$$\boldsymbol{x}_{n+1}(i) = \sum_{j=1}^{N} w_i e^{-(\|\boldsymbol{x}'_n(i) - \boldsymbol{x}'_j(i)\|^2/\sigma)} \tag{17}$$

where

$$x'_n(i) = (1-\varepsilon)\boldsymbol{x}_n(i) + \frac{\varepsilon}{2}(\boldsymbol{x}_n(i+1) + \boldsymbol{x}_n(i-1)) \tag{18}$$

σ is the variance of the Gaussian function [19], and N is the length of the data sequence collected at the lattice i. For (18), Nh is chosen as 1. If Nh is set to zero, then $x'_n(i) = x_n(i)$ and hence (17) becomes the standard temporal RBF predictor. When we choose Nh equal to 2, (18) involves combination of 5 lattices and becomes

$$\begin{aligned} x'_n(i) = &(1-\varepsilon)\boldsymbol{x_n}(i) + \frac{\varepsilon}{2}(\boldsymbol{x_n}(i+1) + \boldsymbol{x_n}(i-1)) \\ &+ \frac{\varepsilon}{4}(\boldsymbol{x_n}(i+2) + \boldsymbol{x_n}(i-2)). \end{aligned} \tag{19}$$

In our analysis reported in the next section, couple RBF lattice with $Nh = 0$, 1 and 2 will be used to extract the spatial temporal pattern of sea scattered signals.

IV. Reconstruction of Spatial Temporal Dynamical Model for Sea Scattered Signals

In order to apply the couple RBF lattice, (17)–(19), to experimental data, the spatial temporal sea scattered signals are fed to the equations to construct an optimal spatial temporal predictor. It is then an optimization problem:

$$\min_{\{\boldsymbol{w}_j, \varepsilon\}} \|x_n(i) - \hat{x}_n(i)\| \tag{20}$$

where $x_n(i)$ is the actual signal at sensor i and time n, and $\hat{x}_n(i)$ is the predicted value using the couple RBF lattice.

The computation of the weights is the most time consuming operation in the modeling process, and its complexity grows polynomial with N, since in order to find the coefficients of the expansion an $N \times N$ matrix has to be inverted. However once the coefficients have been computed, the time needed to evaluate the function at a point grows only linearly in N and this process can easily be parallelized. In many applications the number of training examples can be very large, and the inversion of such a huge matrix is not only formidable but could also be unmeaningful since the probability that a large matrix is ill-conditioned is high. Also, when data are noisy which is usually the case, an approximation of data would be preferable. In (10), the basis on which the function is expanded is given by the set of functions h translated and centered on a set of knots, coincident with the data. The interpolation conditions can be weakened if the number of knots is made lower than the number of data and their coordinates are allowed to be chosen arbitrarily [20]. In this case, denoting with $\boldsymbol{c}_1, \boldsymbol{c}_2, \cdots, \boldsymbol{c}_K$ the coordinates of the K knots ($K < N$) the interpolation condition conditions give the linear system

$$\boldsymbol{y} = \boldsymbol{H}\boldsymbol{w} \tag{21}$$

where H is an $N \times .K$ rectangular matrix given as

$$(\boldsymbol{H})_{ij} = h(\|\boldsymbol{x_i} - \boldsymbol{c_j}\|^2) \qquad i = 1, \cdots, N \quad \text{and} \quad j = 1, \cdots, K. \tag{22}$$

A least squares approach can then be adopted and the optimal solution can be written as

$$\boldsymbol{w} = \boldsymbol{H}^+ \boldsymbol{y} \tag{23}$$

where $\boldsymbol{H}^+$ is the pseudo inverse of $\boldsymbol{H}$ given as

$$\boldsymbol{H}^+ = (\boldsymbol{H}^T \boldsymbol{H})^{-1} \boldsymbol{H}^T. \tag{24}$$

This formulation makes sense if the matrix $\boldsymbol{H}^T\boldsymbol{H}$ is nonsingular, and the existence of the inverse of this matrix has been proven [17]. Another advantage of using rectangular matrix is that adaptive algorithm such as the Least Mean Squares (LMS) algorithm [21] and the Recursive Least Squares (RLS) algorithm [21] can be used to estimate the weights. This further reduced the computational time and the hardware complexity for using this model in signal processing applications. In fact, this spatial temporal model can be mapped onto a neural network structure in the same way as the conventional RBF network. For this study, since the sizes of the data sets are not too large, $\boldsymbol{w}$ is solved by batch pseudo-inverse method based on the singular value decomposition (SVD). One advantage of using SVD is to avoid possible singularity in solving least squares problem.

Another problem is the estimation of the parameter ε. If ε is a free parameter for estimation in the optimization process, the complexity of the process will be greatly increased since the optimization problem will be a nonlinear problem. In other words, (23) cannot be applied directly since $\boldsymbol{H}$ and $\boldsymbol{y}$ contains free parameter, ε, for estimation. To keep the fast adaptive processing capability of the mode, we try to determine ε before computing the weight $\boldsymbol{w}$. To do that, we use the spatial correlation coefficients reported in Section II to determine the spatial coupling effects. For instance, our new choice for the nearest neighbor coupling (18) becomes

$$x'_n(i) = \varepsilon_1 x_n(i) + \varepsilon_2 x_n(i+1) + \varepsilon_3 x_n(i-1) \tag{25}$$

where

$$\begin{aligned} \varepsilon_1 &= \frac{\Phi(i,i)}{\Phi(i,i) + \Phi(i,i+1) + \Phi(i,i-1)} \\ \varepsilon_2 &= \frac{\Phi(i,i+1)}{\Phi(i,i) + \Phi(i,i+1) + \Phi(i,i-1)} \\ \varepsilon_3 &= \frac{\Phi(i,i-1)}{\Phi(i,i) + \Phi(i,i+1) + \Phi(i,i-1)}. \end{aligned} \tag{26}$$

We normalize the spatial correlation coefficients so that they can satisfy (3). Based on the spatial correlation analysis (Fig. 6), this choice for the spatial coupling effect of the CML satisfies the exponentially decaying requirement of (5). Note that the spatial coupling generated by (25) is asymmetric which is different from that of the original CML of (7). We want to stress that the spatially symmetric property is just an assumption to simplify the analysis of the CML but not a requirement for using the model.

In [10], we report the results of applying a RBF predictor to reconstruct the temporal dynamics of sea clutter. We observe not only that RBF can predict the motion of sea clutter accurately and hence is a superior clutter canceller compared to the standard linear predictor, but that it can also be used as an adaptive detector in an ocean environment. In this paper we present some preliminary results of sea scattered signal prediction using the spatial temporal predictor, and compare the results with those obtained by a temporal RBF predictor.

In Figs. 7 and 8, we report the prediction analysis of two data sets. The frequency for these two data sets is 12.22 GHz and 8.05 GHz respectively. Three predictors, using 1 channel, 3 channels and 5 channels, are used for comparison. The 1 channel spatial temporal predictor is just the conventional RBF network prediction. There are 127 samples for each data set. 105 of them are used for training the predictor, and 25 are left for testing. The embedding dimension (i.e., predictor order) for the first and the second data set is 8 and 5, respectively. The number of knots used in the RBF for the two data sets is 40 and 20, respectively. The embedding dimension is determined by observing the smallest prediction errors using different embedding dimension as explained later. The number of knots is determined by trial and error. In this study, recursive prediction is used to evaluate the performance of a predictor. By recursive prediction we mean that after training, one data vector from the testing set is fed to the trained predictor and then the predictor uses the predicted value to continue the prediction for the rest of the testing set. For example, if the prediction order is 5, then the data vector ($x_{106}, x_{107}, x_{108}, x_{109}$, and x_{110}) is fed into the trained predictor and the next predicted value $\hat{x}_{111}$ is produced. This predicted value is used to form a new input vector ($x_{107}, x_{108}, x_{109}, x_{110}$, and $\hat{x}_{111}$) to get the next prediction $\hat{x}_{112}$. The process is continued until the last point x_{127} is reached. The recursive prediction idea was originally used in [14] called iterated prediction. It is usually more difficult than the standard one-step ahead prediction, but it is a more reliable indicator to show whether the model can really capture the dynamics of the underlying process or not.

The waveforms of the recursive prediction using the three predictors are depicted in Figs. 7(a) and 8(a). For the first data set, we find that all three predictors can follow the motion the sea scattered signal, while the 3-channel and 5-channel predictors have the predictions closer to the actual waveform, but the temporal predictor can still capture the trend of the evolution. However, the temporal predictor saturates for the second data set, i.e., a fixed point dynamic, and does not produce an acceptable model for the dynamics of the sea scattered signals. When the spatial effects are incorporated into the predictor, we find that the recursive prediction is greatly improved. Both 3-channel and 5-channel predictors seem to be able to follow the trend of the evolution and follow quite closely with the actual waveform. This observation compromises with the spatial correlation analysis in Section II, in which we find that spatial effect is more important for signal with lower frequency.

The prediction errors of these two data sets are plotted in Figs. 7(b) and 8(b) for comparison. For the first data

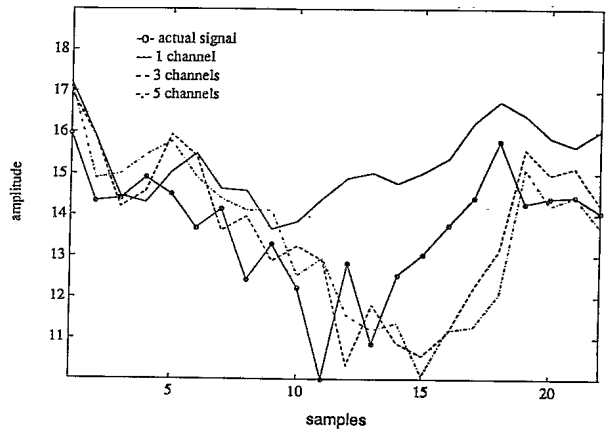

(a)

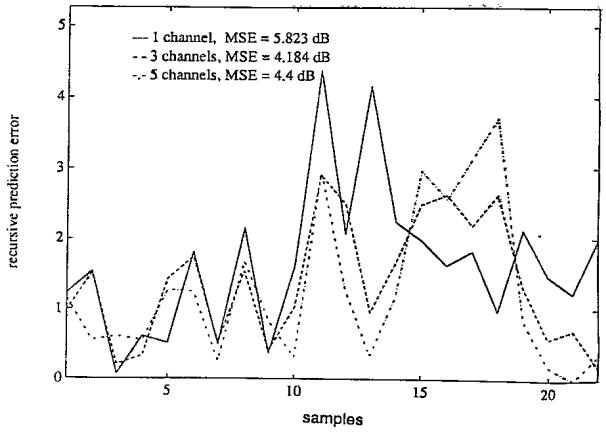

(b)

Fig. 7. (a) Recursive prediction of the first data set, $f = 12.22$ GHz, using 1-channel (pure temporal), 3-channel, and 5-channel couple RBF lattice. (b) Prediction error of the three predictors.

set, 3-channel model has about 1.7 dB improvement to the temporal predictor, and the 5-channel model is about 0.2 dB worse than the 3-channel. This small deficiency of the 5-channel may be the results of including too many insignificant spatial channels for parameter estimation. For the second data set, we find that the spatial correlation affects the prediction performance strongly. The 3-channel predictor has a 4 dB improvement to the temporal predictor, and the prediction error of the 5-channel predictor is about 1.5 dB better than that of the 3-channel predictor.

We also compute the one-step ahead prediction error with different embedding dimension. In our previous study of the chaotic characteristics of sea clutter (radar backscatter from sea surface) [10], we observe that the prediction error will decrease drastically after the embedding dimension passes certain number, and the prediction error will saturate at that level for larger embedding dimensions. That number is also considered as the degree of freedom of the underlying dynamics of the signal sequence. We try to apply the same strategy to the spatial temporal prediction. The results are plotted in Figs. 9 and 10 for the two data sets respectively. We can see that the spatial temporal predictors consistently have better performance than the temporal one. However, all three predictors fail to indicate a suitable embedding dimension as the those observed in [10]

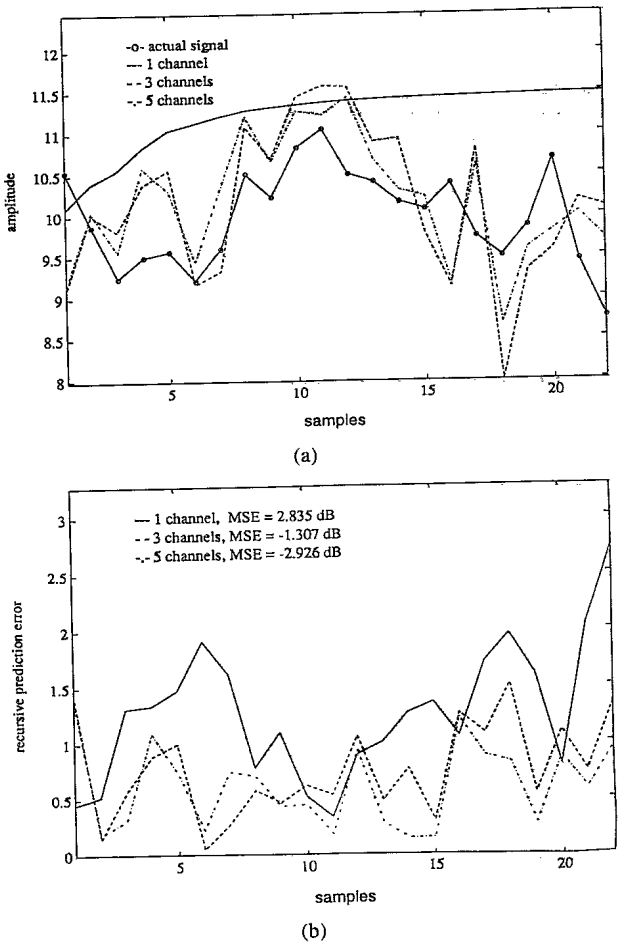

Fig. 8. (a) Recursive prediction of the second data set, $f = 8.05$ GHz, using 1-channel (pure temporal), 3-channel, and 5-channel couple RBF lattice. (b) Prediction error of the three predictors.

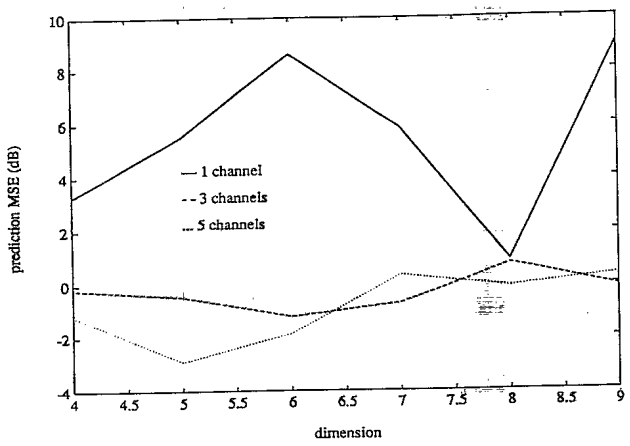

Fig. 9. Plot of one-step ahead prediction errors for the first data set versus embedding dimension.

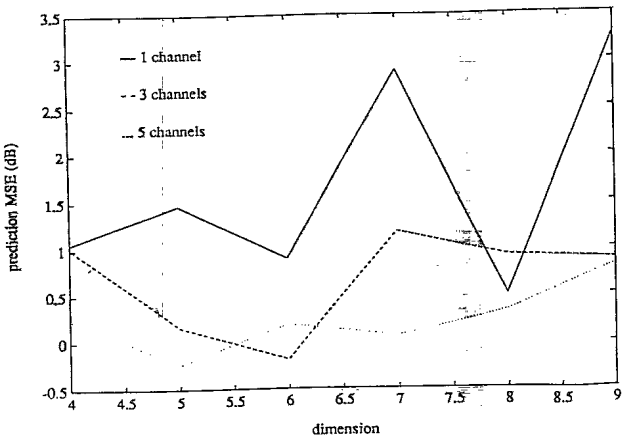

Fig. 10. Plot of one-step ahead prediction errors for the second data set versus embedding dimension.

since no saturation effect is observed. We believe that the main reason is that the data used here is forward sea scattering signals and the length of the data record is much shorter (127 snapshots for each experiment). This is another reason that RBF is used since it is a global interpolation technique with good localization properties.

V. Discussion

Spatial temporal processes, that is, processes that develop simultaneously in space and time, occur in nearly all areas of the applied science [22] including sea scattered signals. Conventional signal processing model for sea scattered signals uses a statistical approach, and ignores the underlying spatial temporal dynamical mechanisms of the process. In this paper a spatial temporal dynamical model, called couple RBF lattice, has been developed as an extension of the temporal RBF neural network. In the previous studies, the RBF neural network is found to provide a good model for sea scattered signals for signal processing applications. Due to the spatial correlation effects, we try to develop a spatial temporal dynamical model for the sea scattered signals. Following the temporal dynamical system reconstruction approach, the couple RBF lattice is used to predict real sea scattered data, and the model is constructed using training algorithm. The complexity of the couple RBF lattice is similar to that of a RBF neural net, and it seems to provide a better model for the sea scattered signals than the RBF network based on the real data used in this study. Based on the spatial correlation analysis and the new spatial temporal predictive analysis, we conclude that spatial correlation is an important factor in modeling sea scattered signals, and the new model provides an accurate description of the sea scattered phenomenon. Our next task is to apply this spatial temporal model to signal processing applications such as spatial temporal beamforming and detection [23], using the same approach that we apply the temporal dynamical model to these problems [9], [10], [24].

References

[1] S. K. Cho, *Electromagnetic Scattering*. Berlin: Springer-Verlag, 1990.
[2] K. D. Ward, C. J. Baker, and S. Watts, "Maritime surveillance radar part 1: Radar scattering from the ocean surface," *Proc. IEE*, vol. 137, pt. F, pp. 51–62, 1990.
[3] K. D. Ward, "A radar sea clutter model and its application to performance assessment," *IEE Conf. Pub. No. 216 (Radar 82)*, pp. 203–207, 1982.
[4] C. J. Baker, J. M. Pink, and R. J. A. Tough, "A statistical model for radar target detection in clutter," *Proc. IEEE Nat. Radar Conf.*, 1988, pp. 241–245.

[5] E. Conte and M. Longo, "Characterization of radar clutter as a spherically invariant random process," *Proc. IEE*, vol. 134, pt. F, pp. 191–197, 1987.
[6] E. Jakeman and R. J. A. Tough, "Non-Gaussian models for the statistics of scattered waves," *Advanced Physics*, vol. 37, pp. 471–529, 1988.
[7] H. Leung, "Experimental modeling of electromagnetic waves scattering from an ocean surface based on chaos theory," *Chaos, Solitons Fractals*, vol. 2, no. 1, pp. 25–43, 1992.
[8] J. D. Farmer and J. J. Sidorovich, "Predicting chaotic time series," *Physical Rev. Lett.*, vol. 59, pp. 845–849, 1987.
[9] H. Leung, T. Lo, and J. Litva, "Angle-of-arrival estimation in multipath environment using chaos," *Signal Processing*, vol. 31, pp. 57–68, 1993.
[10] H. Leung and T. Lo, "Chaotic radar signal processing over the sea," *IEEE J. Oceanic Eng.*, vol. 18, no. 3, pp. 287–295, 1993.
[11] J. P. Crutchfield and K. Kaneko, "Phenomenology of spatial-temporal chaos," in Hao Bai-Lin, Ed.,*Directions in Chaos*. Singapore: World Scientific, 1987, pp. 272–353.
[12] R. Kapral, "Coupled map lattices: Abstract dynamics and models for physical systems," in A. Babloyantz, Ed.,*Self-Organization, Emerging Properties and Learning*. New York: Plenum, 1991, pp. 31–40.
[13] K. Kaneko, "Simulating physics with coupled map lattices," in K. Kawasaki *et al.*, Ed.,*Formation, Dynamics and Statistics of Patterns*, vol. 1 Singapore: World Scientific, 1990, pp. 1–54.
[14] A. Lapedes and R. Farber, "Nonlinear signal processing using neural networks: Prediction and signal modelling," Los Alamos, 1987.
[15] M. Casdagli, "Nonlinear prediction of chaotic time series," *Physica D*, vol. 35, pp. 335–356, 1989.
[16] F. C. Richards, T. P. Meyer, and N. H. Packard, "Extracting cellular automaton rules directly from experimental data," *Physica D*, vol. 45, pp. 189–202, 1990.
[17] C. A. Micchelli, "Interpolation of scattered data: Distance matrices and conditionally positive definite functions," *Constructive Approximation*, vol. 2, pp. 11–22, 1986.
[18] A. Yuille and N. Grzywacz, "The motion coherence theory," in *Proc. Int. Conf. Computer Vision*, Washington, DC, 1988, pp. 344–354.
[19] B. W. Silverman, *Density Estimation for Statistics and Data Analysis*. New York: Chapman and Hall, 1986.
[20] D. S. Broomhead and D. Lowe, "Multivariate functional interpolation and adaptive network," *Complex Systems*, vol. 2, pp. 321–355, 1988.
[21] S. Haykin, *Adaptive Filter Theory*, 2nd ed. Englewood Cliffs, NJ: Prentice-Hall, 1991.
[22] G. Christakos, "On certain classes of spatiotemporal random fields with applications to space-time data processing," *IEEE Trans. Systems, Man, Cybernet.*, vol. 21, no. 4, pp. 861–875, 1991.
[23] B. H. Maranda and J. A. Fawcett, "Detection and localization of weak targets by space-time integration," *IEEE J. Oceanic Eng.*, vol. 16, no. 2, pp. 189–194, 1991.
[24] H. Leung, M. Blanchette, and S. Haykin, "Clutter cancellation and sea ice detection using artificial neural network," in *Proc. SPIE, Appl. Artificial Neural Networks IV*, Orlando, FL, vol. 1965, pp. 312–323, Apr. 1993.

Henry Leung (S'88–M'90) received the B.Math. degree in applied mathematics from the University of Waterloo, Waterloo, ON, Canada, the M.Sc. degree in mathematics from the University of Toronto, Toronto, ON, Canada, and the M.Eng degree in engineering physics and the Ph.D. degree in electrical engineering from McMaster University, Hamilton, ON, Canada, in 1984, 1985, 1986, and 1991, respectively.

In 1990, he was a Research Engineer at the Communications Research Laboratory, McMaster University. In 1991, he joined the Defence Research Establishment, Ottawa ON, Canada as a Defense Scientist. His research interests include adaptive signal processing, neural networks, nonlinear dynamics, and data fusion.

Titus K. Y. Lo (S'85–M'88) received the B.A.Sc. degree in electrical engineering from the University of British Columbia, Vancouver, BC, Canada, and the M.Eng. degree in electrical engineering from McMaster University, Hamilton, ON, Canada, in 1986 and 1989, respectively.

Since 1988, he has been with the Communications Research Laboratory, McMaster University, where he is working as a Research Engineer. His research interests include neural networks, advanced signal processing techniques, and their applications in wireless communications and remote sensing.